

**Web Table 1.** Summary of Demographic Characteristics of Participants in the General Population

Cohort (n = 760), Singapore, 2009–2010.

	<b>N</b>	<b>%</b>
<b>Age group, years</b>		
Below 25	85	11.2
25–34	109	14.3
35–44	222	29.2
45–54	228	30.0
Above 55	116	15.3
<b>Gender</b>		
Male	311	40.9

## Web Appendix 1.

### Reversible Jump Markov Chain Monte Carlo (MCMC)

Let's define the state of the parameter to be  $x = (k, \theta_k)$ , where  $k$  indicates the model index and  $\theta_k$  represents the parameters used in model  $k$ . We define Model 1 as the model when individual  $i$  was not infected, i.e.  $I_i = 0$  and define Model 2 as the model when individual  $i$  was infected, i.e.  $I_i = 1$ . Now consider a move from Model 1 to Model 2. The current state is, therefore,  $x = (1, \theta_1)$  where  $\theta_1 = B_i$ . However, there are no equivalent parameters for  $(M_i, S_i, L_i, T_i)$  in Model 1. To overcome this issue, we generate four random numbers  $u_1, u_2, u_3$  and  $u_4$  independently from four normal distributions  $(g_1, g_2, g_3, g_4)$  with fixed mean and variance. Then the new state of the chain,  $x' = (2, \theta_2)$ , where  $\theta_2 = (B_i, M_i, S_i, L_i, T_i)$ , could be constructed by a diffeomorphic (invertible and differentiable) function  $h$  such that  $(x') = h(x, u_1, u_2, u_3, u_4) = (B_i, e^{u_1}, e^{u_2}, e^{u_3}, u_4)$ . Then the reverse move, i.e. from Model 2 to 1, is derived by setting  $(x, u_1, u_2, u_3, u_4) = h^{-1}(x') = (B_i, \log(M_i), \log(S_i), \log(L_i), T_i)$ . The acceptance probability for the move from Model 1 to 2 is, therefore,

$$\alpha(x, x') = \min\left(1, \frac{\pi(2, \theta_2)}{\pi(1, \theta_1)} (g_1(u_1)g_2(u_2)g_3(u_3)g_4(u_4))^{-1} \left| \frac{\partial(\theta_2)}{\partial(\theta_1, u_1, u_2, u_3, u_4)} \right| \right),$$

and from model 2 to model 1,

$$\alpha(x', x) = \min\left(1, \frac{\pi(1, \theta_1)}{\pi(2, \theta_2)} (g_1(\log(M_i))g_2(\log(S_i))g_3(\log(L_i))g_4(T_i)) \left| \frac{\partial(\theta_1, u_1, u_2, u_3, u_4)}{\partial(\theta_2)} \right| \right).$$

The new candidate for each parameter will be either accepted or rejected using the acceptance probability above. The estimated value for each parameter will be obtained until its posterior distribution reach a stationary distribution.

## Prior distributions and validation of the approach

A hierarchical model for the baseline ( $B_i$ ), peak time ( $M_i$ ), steepness ( $S_i$ ), and peak rise parameter ( $R_i$ ) was built using independent log Normal priors, for instance  $\log(B_i) \sim N(\mu_B, \sigma_B^2)$  etc. Each pair of hyperparameters, e.g.  $(\mu_B, \sigma_B^2)$ , was given a non-informative normal-inverse gamma prior distribution which facilitated a Gibbs sampler from the conjugate conditional distribution. The prior distributions for all other parameters were taken to be uniform distributions over their support regions.

The infection status  $I_i$ , was proposed from a Bernoulli (0.5) distribution via the Metropolis-Hastings algorithm. All other parameters were proposed independently using normal distributions centered on the current value with bandwidth selected from pilot runs, and  $T_i$  rounded to the nearest integer.

Parameters were estimated with 10,000 iterations after a burn-in period of 2000. Posterior distributions of the model parameters showed good convergence that was assessed using trace plots and the Geweke diagnostic.(1)

To validate the inference routine, we took the same cohort size and the best guess for each parameter to generate a simulated set of data points for each individual, and we then fitted the same model on the simulated dataset. Model accuracy was checked by comparing the estimated means and 95% credible intervals (CrIs) with the parameters used to simulate data.

## Web Appendix 2. Statistical model for epidemic simulation

We assumed that infected individuals would remain infectious for 7 days and would not have reinfections within 30 days from disease onset, following which infection risk is modulated by the simulated titer. The model was based on a population with size of 1,000 over a period of 10 years. The pre-infection geometric mean titers (GMT) for each individual at the beginning of the first pandemic wave followed uniform distributions on the interval [0, 1]. The risk of infection for a susceptible individual  $i$  at day  $t$  was given by  $p_{it}$ , which was derived from a discrete time approximation to a continuous infection rate. We assumed that there was an exponential decay in the population at risk over time, so  $p_{it}$  can be derived using the formula below:

$$p_{it} = \begin{cases} [1 - e^{-(\alpha + \beta NI_t) \times s_t}] \times e^{\theta \times \text{titer}_{it}} & \text{if no prior infection within the last 30 days} \\ 0 & \text{otherwise} \end{cases}$$

where  $NI_t$  is the number of infections over the last 7 days,  $s_t$  gives the effect of seasonal forcing at day  $t$ ,  $\theta$  determines the protective effect conferred by antibody titers which was taken from Zhao et al.,  $\text{titer}_{it}$  is the antibody titers for individual  $i$  at time  $t$ , and  $\alpha$  and  $\beta$  capture importation and autochthonous infection, respectively. We gave values of 0.1 and 0.3 for  $\alpha$  and  $\beta$  respectively because it could produce a similar pattern for the first influenza pandemic wave and two subsequent waves in Singapore. If individual  $i$  was infected at day  $t$ , his/her antibody titers would be boosted by adding the estimated mean post-infection titers (Figure 4A) to the baseline titer. Seasonal forcing was considered by multiplying the infection risk by a sinusoidal term  $s_t = e^{\gamma \times \sin(\frac{2\pi t}{365})}$ , where  $\gamma$  determines the amplitude of the oscillation

**Web Table 2. Comparison of pre-infection titer distributions between the community cohort and RT-PCR cohort.**

<b>Pre-infection titer</b>	<b>Community cohort n = 199* (%)</b>	<b>RT-PCR cohort n = 76* (%)</b>
<b>&lt;1:20</b>	194 (97.4)	71 (93.4)
<b>≥1:20</b>	5 (2.6)	5 (6.6)
<b>P-value obtained from the Fisher's exact test</b>	0.15	

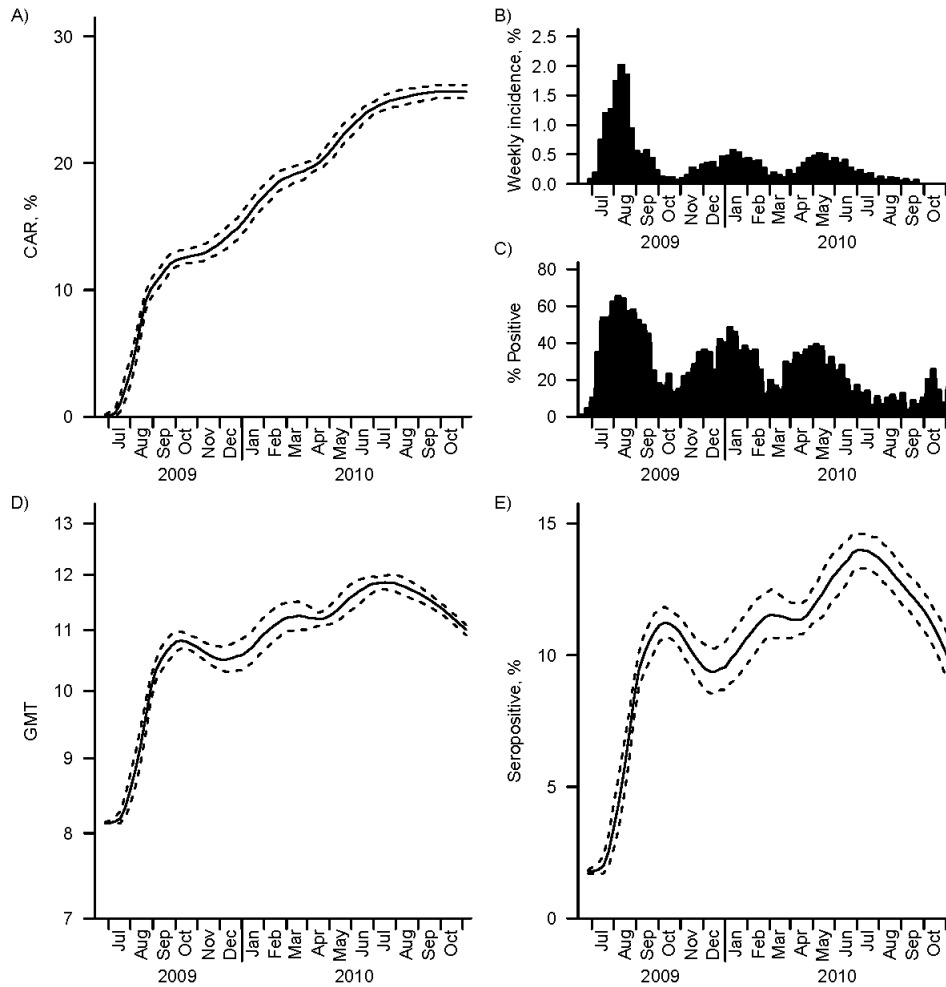
**\*There were 208 of 760 estimated influenza A(H1N1)pdm09 cases in the community cohort. Of which 199 had pre-infection titers measured and 76 of 118 RT-PCR cases having pre-infection titers measured.**

**Web Table 3. Posterior means of population parameters with 95% credible intervals obtained from models using observed data and simulated data.**

	Posterior mean (95% CrIs)			Posterior mean (95% CrIs)	
	Parameter used for simulation	Inference		Parameter used for simulation	Inference
$\mu_B$	-0.54	-0.54 (-0.57, -0.50)	$\nu_B$	0.24	0.24 (0.22, 0.26)
$\mu_R$	4.82	4.81 (4.76, 4.86)	$\nu_R$	0.59	0.58 (0.53, 0.64)
$\mu_M$	1.28	1.28 (1.19, 1.38)	$\nu_M$	2.15	2.14 (1.95, 2.35)
$\mu_S$	3.38	3.38 (3.31, 3.45)	$\nu_S$	1.19	1.18 (1.08, 1.30)
$\phi$	-5.42	-5.24 (-5.57, -5.29)			

**Web Table 4.** Estimated means of overall and age-stratified cumulative attack rates (CARs) with 95% credible intervals (CrIs) at the end of first and third wave, Singapore, 2009–2010.

	End of first wave (mid-October 2009)		End of third wave (July 2010)	
	mean	95% CrI	mean	95% CrI
<b>Overall CAR</b>	12.7%	12.2% to 13.2%	23.8%	23.2% to 24.5%
<b>Age-stratified CAR</b>				
Below 25	20.7%	20.0% to 22.4%	38.2%	35.3% to 41.2%
25–34	9.2%	8.3% to 10.1%	22.4%	22.0% to 23.9%
35–44	13.1%	12.6% to 14.4%	22.0%	20.7% to 23.0%
45–54	12.7%	11.8% to 13.6%	22.5%	21.5% to 23.7%
Above 55	9.4%	8.6% to 10.3%	20.7%	19.0% to 22.4%



**Web Figure 1. Population level dynamics for the cumulative attack rates (CAR) (A), observed and modelled influenza A(H1N1)pdm09 incidence (B), geometric mean titers (C) and seropositive rate (D) over time using model with fluctuating risk of infection over time.** For panel A), C) and D), the solid line on each panel represent the estimated mean values and the dotted lines represent the 95% credible intervals (CrI). On panel B), the top subpanel illustrates the modelled incidence of influenza A(H1N1)pdm09 infections (black bars), and the bottom subpanel illustrates the observed relative proportions of influenza A(H1N1)pdm09 infections among influenza-like illness (ILI) samples obtained from the routine primary care surveillance (grey bars). The y-axis scales differ for these two subpanels on panel B).



### **Web Appendix 3. Discussion on the consistency of results**

The finding that antibody titers peak 6–7 weeks after infection is consistent with the results from previous studies that report that peak levels were achieved 4–7 weeks after influenza infection/vaccination.(2–5) We also found that antibody titers against pandemic influenza A(H1N1) dropped rapidly to half their peak level 5–8 months after infection followed by a slower decrease until one year post infection (beyond which we could not accurately estimate). This finding supports the results from historical studies that a faster decrease in antibody titers was observed within the first 6 months.(6–8) However, different opinions exist pertaining as to the time interval for the half-life of antibody titers. A pioneering immunological study by Horsfall et al. in 1941 found that the half-life for influenza antibody titres post-infection is 2–3 months among 5 study subjects.(9) In a more recent study from South Korea, antibody titers were measured up to 12 months following vaccination with standard-dose, inactivated, trivalent influenza vaccine.(10) For younger adults (<65 years) titers similar to 4 weeks post-vaccination persisted till 6 months, but approached pre-vaccination levels at 12 months. In older adults, HAI titers decayed to below seroprotective levels by 6 months. The shorter half-life time observed in the Horsfall study could be a reflection of small sample size (n = 5) and concomitant sampling error. Moreover, it has been demonstrated that naturally acquired influenza antibodies persist longer than artificially acquired (i.e. vaccine induced) influenza antibodies.(11,12)

**Web Table 5. A comparison between the time window between two consecutive blood samples and uncertainty time interval for estimated time of infection.** The distribution for both time intervals are skewed so median with interquartile range were reported.

	Sample size	Median time interval between blood samples, days (IQR)	Median uncertainty interval for estimated time of infection, days (IQR)
Sample 1 — Sample 2	91	10 (9, 42)	9.8 (4.3, 34.2)
Sample 2 — Sample 3	35	7 (6, 34.7)	17.1 (5.8, 70.3)
Sample 3 — Sample 4	45	26 (11, 28)	20.8 (9.8, 49.9)
Sample 4 — Sample 5	27	12 (10.7, 24.4)	12 (11.2, 13)
Sample 5 — Sample 6	8	12 (11.2, 13)	26.3 (21.6, 47.4)

## Reference

1. Geweke J. Evaluating the accuracy of sampling-based approaches to the calculation of posterior moments. In: Bernardo JM, Berger JO, Dawid AP, et al., eds. *Bayesian Statistics 4: Proceedings of the Fourth Valencia International Meeting*. Oxford: Oxford University Press; 1992:163–193.
2. Couch RB, Kasel JA. Immunity to Influenza in Man. *Annu. Rev. Microbiol.* 1983;37(1):529–549.
3. Cauchemez S, Horby P, Fox A, et al. Influenza Infection Rates, Measurement Errors and the Interpretation of Paired Serology. *PLoS Pathog.* 2012;8(12):e1003061.
4. Skowronski DM, Tweed SA, Tweed SA, et al. Rapid Decline of Influenza Vaccine—Induced Antibody in the Elderly: Is It Real, or Is It Relevant? *J. Infect. Dis.* 2008;197(4):490–502.
5. Rastogi S, Gross PA, Bonelli J, et al. Time to peak serum antibody response to influenza vaccine. *Clin. Diagn. Lab. Immunol.* 1995;2(1):120–121.
6. Wright PF, Sannella E, Shi JR, et al. Antibody responses after inactivated influenza vaccine in young children. *Pediatr. Infect. Dis. J.* 2008;27(11):1004–1008.
7. Hsu JP, Zhao X, Chen MI-C, et al. Rate of decline of antibody titers to pandemic influenza A (H1N1-2009) by hemagglutination inhibition and virus microneutralization assays in a cohort of seroconverting adults in Singapore. *BMC Infect. Dis.* 2014;14(1):414.
8. Sacadura-Leite E, Sousa-Uva A, Rebelo-de-Andrade H. Antibody response to the influenza vaccine in healthcare workers. *Vaccine.* 2012;30(2):436–441.

9. Horsfall FL, Rickard ER. NEUTRALIZING ANTIBODIES IN HUMAN SERUM AFTER INFLUENZA A : THE LACK OF STRAIN SPECIFICITY IN THE IMMUNOLOGICAL RESPONSE. *J. Exp. Med.* 1941;74(5):433–439.
10. Song JY, Cheong HJ, Hwang IS, et al. Long-term immunogenicity of influenza vaccine among the elderly: Risk factors for poor immune response and persistence. *Vaccine.* 2010;28(23):3929–3935.
11. Suguitan AL, Zengel JR, Jacobson S, et al. Influenza H1N1pdm-specific maternal antibodies offer limited protection against wild-type virus replication and influence influenza vaccination in ferrets. *Influenza Other Respir. Viruses.* 2014;8(2):169–176.
12. Chan K-H, To KKW, Hung IFN, et al. Differences in antibody responses of individuals with natural infection and those vaccinated against pandemic H1N1 2009 influenza. *Clin. Vaccine Immunol. CVI.* 2011;18(5):867–873.